High-dimensional imaging of the HPV-induced tumor microenvironment to improve clinical outcomes

Abdulrahman, Z.

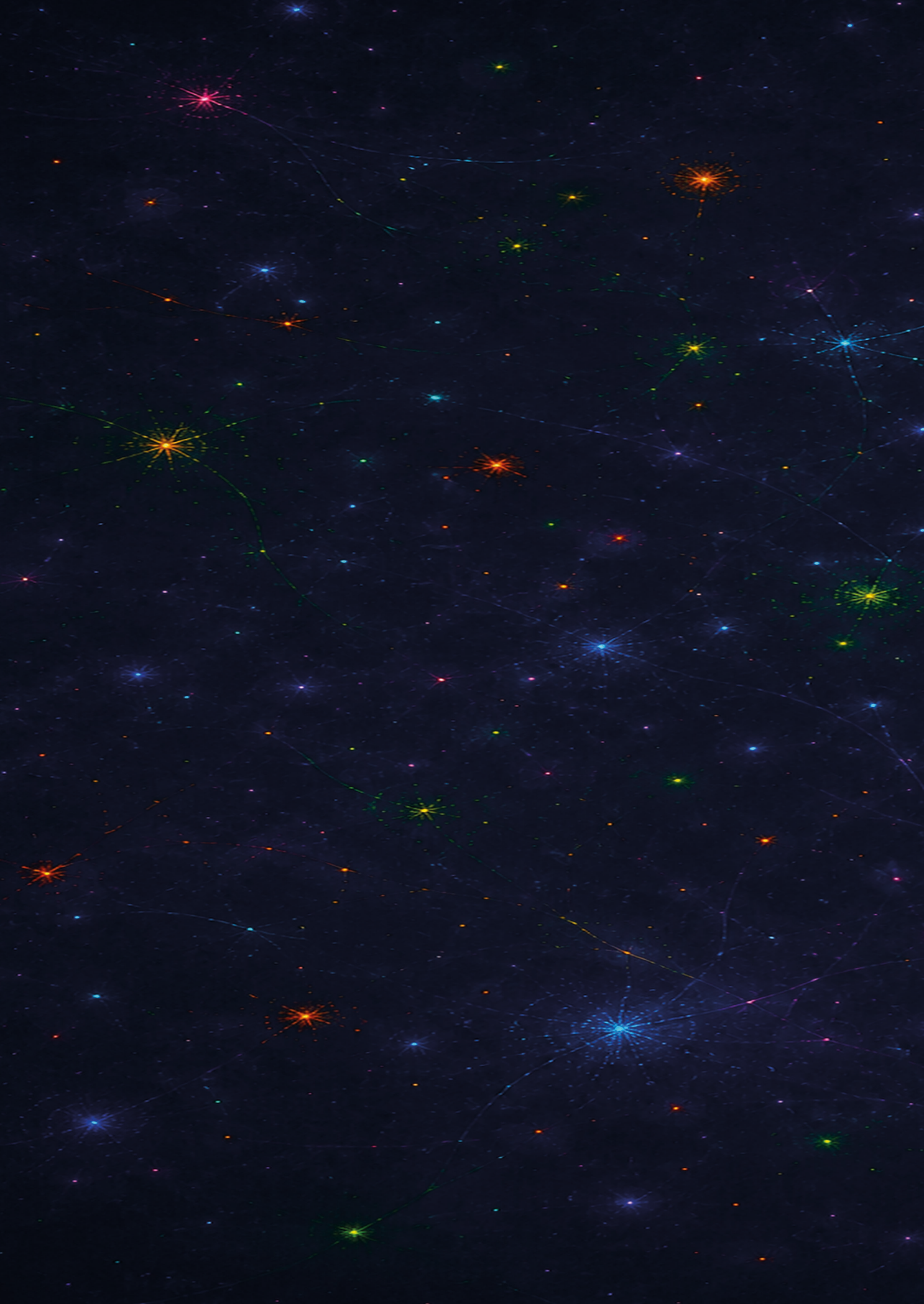

Chapter 3

Pre-existing inflammatory immune microenvironment predicts the clinical response of vulvar high-grade squamous intraepithelial lesions to therapeutic HPV16 vaccination

Ziena Abdulrahman, Noel F.C.C. de Miranda, Edith M.G. van Esch, Peggy J. de Vos van Steenwijk, Hans W. Nijman, Marij J.P. Welters, Mariette I.E. van Poelgeest, Sjoerd H. van der Burg

Journal for ImmunoTherapy of Cancer 2020

Abstract

Background

Vulvar high-grade squamous intraepithelial lesion (vHSIL) is predominantly induced by high-risk Human Papilloma Virus type 16 (HPV16). In two independent trials, therapeutic vaccination against the HPV16 E6 and E7 oncoproteins resulted in objective partial and complete responses in half of the HPV16$^+$ vHSIL patients at 12 months follow-up. Here, the pre- and post-vaccination vHSIL immune microenvironment in relation to the vaccine-induced clinical response was investigated.

Methods

Two novel seven-color multiplex immunofluorescence panels to identify T cells (CD3, CD8, Foxp3, Tim3, Tbet, PD-1, DAPI) and myeloid cells (CD14, CD33, CD68, CD163, CD11c, PD-L1, DAPI) were designed and fully optimized for formalin-fixed paraffin-embedded tissue. 29 pre- and 24 post-vaccination biopsies of vHSIL patients, and 27 healthy vulva excisions, were stained, scanned with the Vectra multispectral imaging system, and automatically phenotyped and counted using inForm advanced image analysis software.

Results

Healthy vulvar tissue is strongly infiltrated by CD4 and CD8 T cells expressing Tbet and/or PD-1 and CD14$^+$HLA-DR$^+$ inflammatory myeloid cells. The presence of such a coordinated pre-existing pro-inflammatory microenvironment in HPV16$^+$ vHSIL is associated with complete response after vaccination. In partial responders, a disconnection between T cell and CD14$^+$ myeloid cell infiltration was observed, whereas clinical non-responders displayed overall lower immune cell infiltration. Vaccination improved the coordination of local immunity, reflected by increased numbers of CD4$^+$Tbet$^+$ T cells and HLA-DR$^+$CD14$^+$ expressing myeloid cells in patients with a PR or CR, but not in NR patients. CD8$^+$ T cell infiltration was not increased after vaccination.

Conclusion

A pre-vaccination inflamed type 1 immune contexture is required for stronger vaccine-induced immune infiltration and is associated with better clinical response. Therapeutic vaccination did not overtly increase immune infiltration of cold lesions.

Introduction

The immune system is key to the control of tumor outgrowth. A dense infiltration with type 1 $CD4^+$ and $CD8^+$ T cells in the tumor microenvironment (TME) is prognostic for longer survival and associated with a favorable response to therapy in many but not all cancers.[1,2] Several effective strategies, including adoptive cell transfer[3,4] and immune checkpoint blockade[5,6] demonstrated the power of immunotherapy in cancer, making it one of the pillars of modern cancer therapy in the clinic. With the widespread testing of these immunotherapies, it has become clear that their success builds on the presence of pre-existing tumor infiltrating T cells, since both their absence and their incapability to infiltrate the tumor cell nests are associated with lack of response after immunotherapy.[7, 8] Hence, for those patients there is a need for treatment modalities that can stimulate tumor-reactive T cell immunity and/or promote their infiltration into tumors. Here, cancer vaccines come into play, since they can increase the magnitude and width of the tumor-reactive T cell pool by stimulating both the naive T cell repertoire and the existing tumor-specific T cell population. In a recent review at least 18 trials were identified to report regression of premalignant lesions or tumors after vaccination with a series of different antigens over a spectrum of different solid tumors. In general, patients with a clinical response showed a robust or more active type 1 T cell response.[9] In view of the fact that cancer immunity is influenced by a complex set of host, tumor and environmental factors[10, 11] it was no surprise that vaccine-induced tumor regression was only observed in a few patients per trial.[9]

About 20% of human cancers are induced by viruses.[12] Human Papillomavirus type 16 (HPV16) is a high-risk DNA virus which causes anogenital and oropharyngeal (pre-)cancers. To increase T cell reactivity against HPV16 caused diseases, two DNA vaccines and one synthetic long peptide (SLP) vaccine have been developed to harness the immune system against the HPV16 encoded oncoproteins E6 and E7.[13-16] Immunization with these vaccines resulted in the induction of potent $CD4^+$ T helper type 1 (Th1) responses and $CD8^+$ cytotoxic T cell responses in patients with HPV16-induced precancerous cervical lesions[15-18] and precancerous vulvar lesions (vHSIL)[19-21]. Importantly, these vaccines were able to induce partial and complete regression of the lesions in a substantial number of vaccinated patients.[19-22] More recently ISA101, an HPV16 synthetic long peptide (SLP) vaccine, showed strong biological signs of clinical activity in patients with either HPV16-positive oropharyngeal or cervical cancer.[23-24] The HPV-specific T cell response after vaccination, as measured in the blood

of patients, was strongly correlated to clinical outcome.[19-22, 24, 25] Despite these correlations there are still a number of patients who, based on their vaccine-induced immune response, were expected to show a clinical response but failed to do so. There may be a multitude of reasons for this, but inspired by the studies showing that checkpoint blockade is specifically successful in patients with pre-existing T cell inflamed tumors[10, 11], we hypothesized that this may also hold true for therapeutic cancer vaccination.

In order to address this question, we studied a group of patients treated with ISA101, about 50% of whom showed an objective regression of their HPV16-induced vHSIL.[21] Based on our previous studies of the TME in vHSIL, demonstrating the impact of different types of immune cells on the recurrence rate of vHSIL[26, 27], two antibody panels for studying T cells and myeloid cells were designed and fully optimized for multispectral immunofluorescence imaging, hereby enabling unprecedented in-depth characterization of the immune composition in the TME of vHSIL biopsies before and after vaccination, and in healthy vulvar tissue for comparison. Our data revealed that complete responders to vaccination had a strong and coordinated pre-existing infiltration with type 1 T helper cells and inflammatory ($CD14^+$) myeloid cells, similar to what was found in healthy vulvar tissue. In contrast, clinical non-responders displayed an intrinsic incapacity to attract immune cells as they displayed much lower overall infiltration before vaccination and this was not increased after vaccination.

Materials and Methods

Patient materials

Pre- and post-vaccination formalin-fixed paraffin-embedded (FFPE) biopsies of 29 women of ≥18 years old with histologically confirmed HPV16+ vHSIL were taken. These women participated in a phase I/II therapeutic HPV16 SLP vaccination trial with ISA101.[21] The ISA101 vaccine was injected subcutaneously and consists of 13 SLPs covering the entire amino acid sequence of HPV16 oncoproteins E6 and E7, dissolved in dimethylsulfoxide in 20 mM of phosphate-buffered saline and emulsified with Montanide adjuvant (ISA-51 Seppic). Clinical efficacy assessments in the trial were performed at 3 and 12 months after the fourth and last vaccination. The patients were grouped into the best clinical response at 12 months after vaccination without additional treatment: complete responders (CR) when the lesion completely disappeared, partial responders (PR) when ≥50% of the total lesion area had disappeared, and non-responders

(NR) when <50% of the lesion had disappeared. The presence of HPV16 DNA in the lesion was determined by HPV16 PCR analysis. Furthermore, FFPE healthy HPV-negative vulvar tissue from 27 anonymous women who underwent labia reduction surgery was included. All patients gave written informed consent. The study was conducted in accordance with the Declaration of Helsinki and approved by the national Central Committee on Research Involving Human Subjects (CCMO, NL21215.000.08) and the local institutional ethical committee (P08.197).

Multiplex immunofluorescence imaging

The specificity of each primary antibody was first assessed with immunohistochemistry, tonsil slides served as positive and negative control. After selection of the best primary antibodies, the immunodetection conditions for each marker in seven color immunofluorescence were optimized. Dim markers were tyramide signal amplified with Opal to enable their detection by fluorescence microscopy, and primary antibodies with clashing species and isotypes in the panel were directly labeled with fluorochromes or detected with species/isotype-specific antibodies.[28] A complete overview of the design of the T cell panel and myeloid cell panel is presented in **Supplemental Files 1 and 2**, respectively. In the seven color immunofluorescent procedure, 4um FFPE tissue sections were deparaffinized, endogenous peroxidase was blocked with hydrogen peroxide, and heat induced epitope retrieval was performed with citrate (10mM, pH 6.0) in the T cell panel and with tris-EDTA (10mM/1mM, pH 9.0) in the myeloid cell panel. Non-specific binding sites were blocked with SuperBlock (ThermoFisher Scientific). First, the antibodies detected by Opal were applied and subjected to the recommended tyramide signal amplification protocol, followed by the unconjugated antibodies which were incubated overnight. On the second day, after detection of the previous with respective fluorescently labelled secondary antibodies, the directly labeled primary antibodies were incubated for 5 hours and, lastly, DAPI was applied as nuclear counterstain.[28]

Quantification of immune cells in the TME

Immunofluorescence images were acquired with the Vectra 3.0.5 multispectral imaging microscope (PerkinElmer) at 20x magnification and exposure times were set to avoid spectral overlap. Immune cells in the TME were automatically phenotyped and counted with inForm 2.4 image analysis software (PerkinElmer), after manual training and validation of procedures. The software was trained to segment epithelial and stromal fractions, segment DAPI+ nucleated cells, and to assign a phenotype to each cell **(Supplemental File 3a)**. All images

were visually inspected on accurateness in segmenting tissue and phenotyping cells, and if errors were detected the training was further optimized. Given the multitude of possible co-expressed markers, each seven color panel was divided into multiple sub-analyses **(Supplemental File 3b)** to preclude the exclusion of relevant phenotypes, after which the phenotypes of the different sub-analyses were merged per cell based on X,Y-positions to obtain the full seven marker expression profile of each cell. Immune cell counts were normalized for tissue size (cells/mm^2 epithelium and cells/mm^2 stroma). After merging all sub-analyses, a threshold of a median cell count ≥ 10 cells/mm2 was applied to enable the analysis of relevant phenotypes.

Statistical analysis

Statistical data analysis was performed with SPSS 25.0 (IBM Corporation). Immune counts of two groups were compared with the non-parametric Mann-Whitney U test. Pearson correlation was used to study correlations between the T cell infiltrate and the myeloid cell infiltrate in each group (clinical non-responders, partial responders, complete responders and healthy donor vulva). Two sided p-values <0.05 were marked as significant. GraphPad Prism 8.0.1 (GraphPad Software Inc.) was used to create graphs.

Results

Healthy vulvar tissue is predominantly infiltrated by type 1 activated T cells and inflammatory macrophages

Correct interpretation of the immune infiltration in precancerous vulvar lesions requires a profound understanding of the immune microenvironment in healthy vulvar tissue. In-depth characterization of the immune infiltrate was performed with two panels of antibodies to identify different subsets of T cells and myeloid cells in the epithelium and stroma, using multispectral immunofluorescence imaging (**Figure 1ab and Supplemental File 4**). Analysis of 27 healthy HPV-negative vulvar tissues revealed that normal vulvar tissue is strongly infiltrated with T cells and myeloid cells, albeit at variable levels between individuals (**Figure 2a and Supplemental File 5**). The intraepithelial infiltrate was dominated by type 1 Th cells ($CD3^+CD8^-Foxp3^-$) expressing Tbet and a smaller fraction of which also expressed PD-1 as well as by inflammatory myeloid cells ($CD14^+$ cells). A similar pattern was observed in healthy vulvar stroma, however, here also high numbers of M1 ($CD68^+CD163^-$) and M2 ($CD68^+CD163^+$) macrophages were found and the number of inflammatory

myeloid cells (CD14^{+}) superseded any other immune cell count by far. This data suggests that healthy vulvar tissue is a highly inflammatory microenvironment comprising many type 1 (Tbet^{+}) and activated (PD-1^{+}) T lymphocytes and inflammatory macrophages.

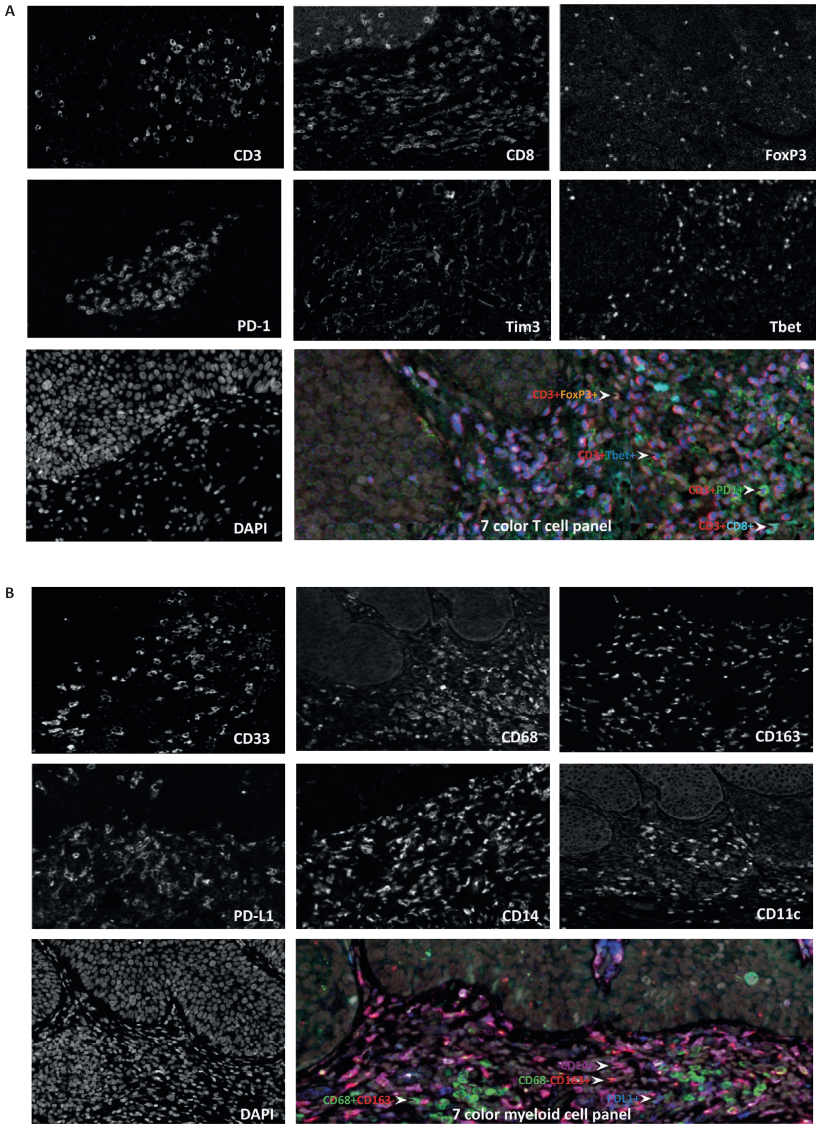

Figure 1. Multiplex immunofluorescence staining to detect T cells and myeloid cells.

Two multiplex panels were developed to detect T cells and myeloid cells in vulvar tissue.
***A**) The expression of each of the 7 markers for T cells showing CD3, CD8, FoxP3, Tbet, Tim3, PD-1 and DAPI as well as a figure showing all 7 markers simultaneously. Arrows indicate examples of analyzed phenotypes. **B**) The expression of each of the 7 markers for myeloid cells showing CD33, CD68, CD163, PD-L1, CD14, CD11c and DAPI as well as a figure showing all 7 markers simultaneously. Arrows indicate examples of analyzed phenotypes.*

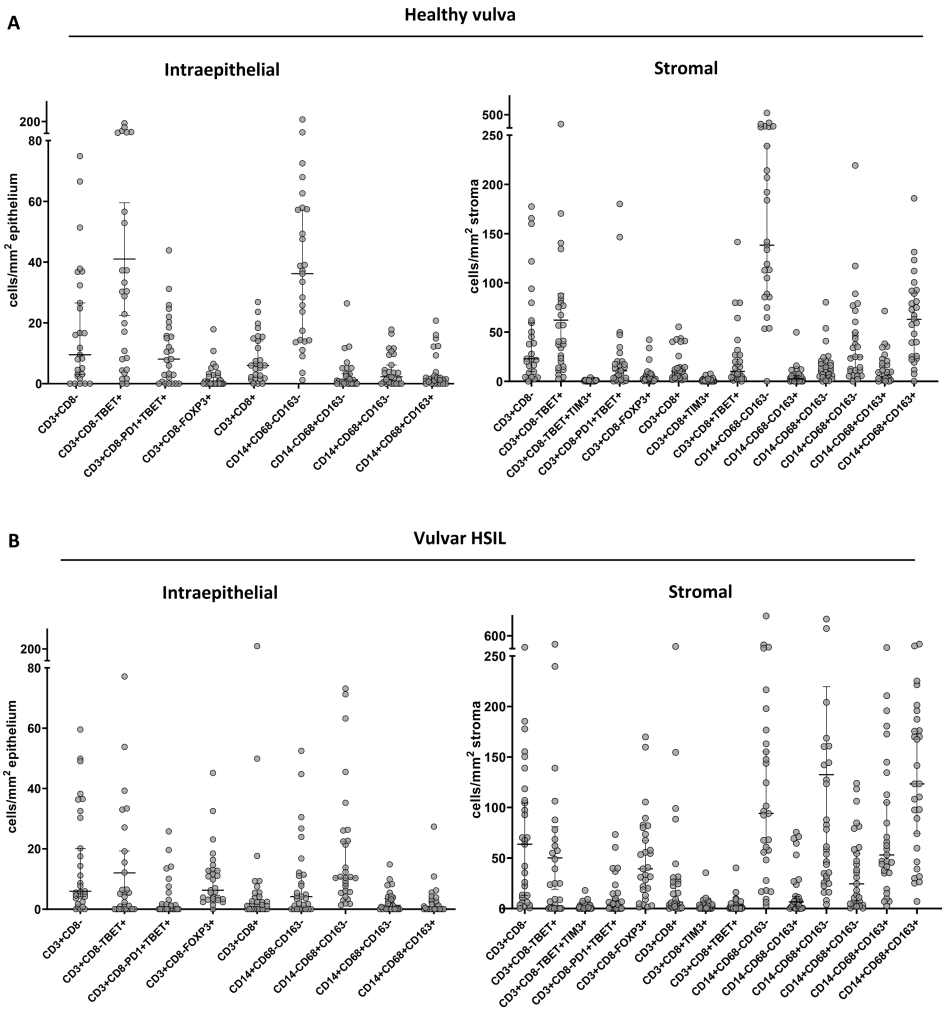

Figure 2. Healthy vulvar tissue is infiltrated by activated type 1 T cells and several types of myeloid cells while the vHSIL immune infiltrate is highly heterogenic amongst different patients.

*The numbers of intraepithelial and stroma infiltrating T cell and myeloid cell subtypes, of which the median cell count exceeded the threshold of ≥ 10 cells/mm2, are presented as cells/mm² for **A**) HPV-negative healthy vulva (n=27) and **B**) vHSIL (n=29) before vaccination. Each dot represents an individual sample, the horizontal bars indicate the median cell counts, the vertical bars are the 95% confidence intervals.*

Strong variations in the lymphoid and myeloid immune infiltration of pre-vaccination vHSIL

We were able to include 29 of the 34 vaccinated vHSIL patients[21] for the current analysis **(Table 1**). Two patients could not be included due to unavailability of FFPE tissue and three due to unknown response 12 months after vaccination. Analyses of the multispectral immunofluorescence imaging for T cells and

myeloid cells revealed that despite the same etiology, the 29 vHSIL patients formed a heterogeneous group as the counts of immune cells infiltrating the epithelium and stroma strongly differed per patient **(Figure 2b and Supplemental File 6).** The overall pattern of intraepithelial and stromal immune cell infiltration resembled that found in healthy tissue. However, whilst 55% of the healthy vulvar tissue-infiltrating $CD14^+$ myeloid cells expressed HLA-DR, this was only 26% in the vHSIL group **(Supplemental File 7).**

Table 1. Patient characteristics pre-vaccination and best clinical response during 12 months follow-up after therapeutic HPV16 SLP vaccination.

Patient study number	Lesion size (cm^2)	Histology	HPV16	Best response without additional treatment	Pre-vaccination biopsy analyzed	3 months post-vaccination biopsy analyzed
1	15,5	VIN3	+	PR	+	+
3	3,0	VIN2	+	CR	+	-*
6	8,0	VIN3	+	PR	+	+
9	3,5	VIN3	+	CR	+	+
10	4,0	VIN2	+	PR	+	+
11	25,3	VIN3	+	NR	+	+
14	0,3	VIN3	+	CR	+	+
15	2,0	VIN2	+	NR	+	+
18	2,0	VaIN3	+	NR	+	+
19	4,5	VIN3	+	NR	+	+
20	2,0	VIN2	+	PR	+	+
21	6,5	VIN3	+	NR	+	-
22	2,0	VIN3	+	NR	+	+
24	6,2	VIN3	+	NR	+	+
26	1,0	VIN2	+	NR	+	+
28	9,5	VIN3	+	NR	+	+
29	4,2	VIN2	+	PR	+	+
30	10,3	VIN3	+	PR	+	-
32	1,5	VIN3	+	CR	+	-*
51	19,0	VIN2	+	NR	+	+
52	120,0	VIN3	+	NR	+	+
53	42,0	VIN3	+	PR	+	+
55	104,0	VIN3	+	PR	+	+
57	3,0	VIN3	+	NR	+	+
58	44,0	VIN3	+	CR	+	-*
59	8,0	VIN3	+	NR	+	+
61	12,0	VIN3	+	CR	+	+
62	3,0	VaIN3	+	PR	+	+
63	3,0	VIN3	+	PR	+	+

NR=no response (<50% lesion size reduction), PR=partial response (≥50% lesion size reduction), CR=complete response (100% lesion clearance). The data were extracted from our previous report.[21]
**vHSIL already cleared in biopsy*

The vHSIL patients were grouped according to their best clinical response obtained without additional treatment during the 12 months follow-up, into CR (n=7), PR (n=10) or NR (n=12). Plots of the data according to clinical outcome revealed a stepwise increase in the median number of intraepithelial and stromal $CD8^+$ T cells, $CD4^+$ ($CD3^+CD8^-Foxp3^-$) $Tbet^+$ Th cells and $CD14^+$ inflammatory myeloid cells as clinical outcome improved, while that of Tregs stepwise decreased (**Figure 3a and Supplemental File 6**). In order to ensure that the $CD3^+CD8^-$ T cells were indeed $CD4^+$ T cells, we analyzed a subset of NR, PR an CR patients for the expression of $CD3^+$, $CD4^+$ and $CD8^+$, confirming that on average 99% of the $CD3^+CD8^-$ T cells were $CD4^+$ T cells (**Supplemental File 8)**. Interestingly, the immune infiltration of pre-vaccination vHSIL in the CR group most closely resembled that of healthy vulvar tissue, whereas this was the opposite for the NR group.

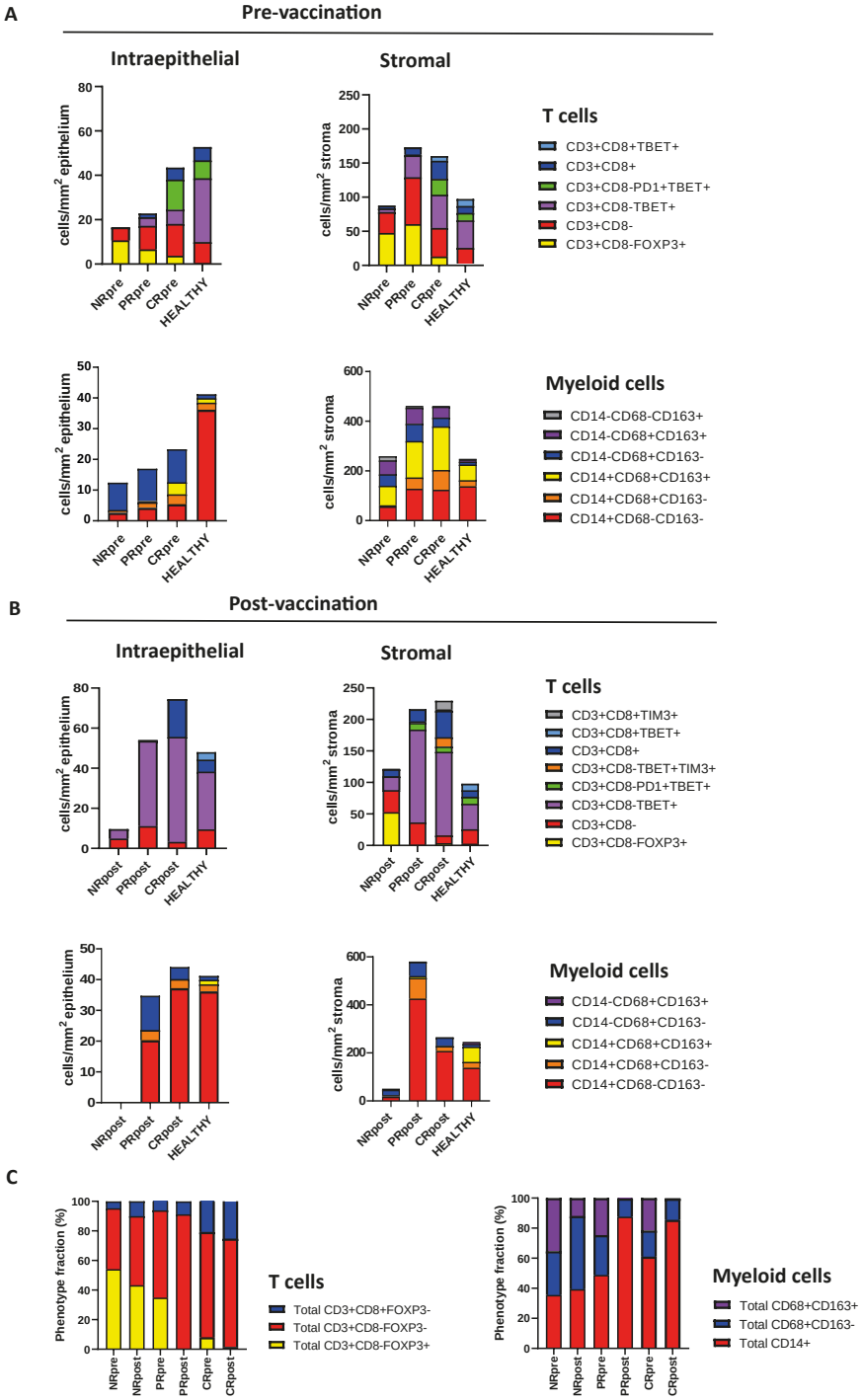

Figure 3. The TME of complete responders displays a similar immune infiltration pattern as found in healthy vulvar tissue.

*The numbers of intraepithelial and stroma infiltrating T cell and myeloid cell subtypes, of which the median cell count exceeded the threshold of ≥ 10 cells/mm2, are presented as cells/mm^2 in the **A**) pre-vaccination (n=29) and **B**) post-vaccination (n=24) vHSIL biopsies of vaccinated patients grouped according to their best clinical response during the 12 months of follow-up, and compared to healthy vulvar tissue (n=27). CR=complete responders (n=7); PR=partial responders (n=10); NR=non-responders (n=12)). Statistical differences in the cell types between patient groups are depicted in Supplemental Files 6 and 9. **C**) Highlighted T cell and myeloid cell subtypes that significantly differed amongst different response groups, shown as fractional differences in all CD3$^+$ T cells (left) or all CD14$^+$ and CD68$^+$ myeloid cells (right), pre- and post-vaccination.*

Coordinated high infiltration with CD4 and CD8 type 1 T cells and inflammatory myeloid cells identifies the complete responders to therapeutic vaccination

To gain a better insight in the coordination of the local immune response, we plotted the correlation between the absolute intraepithelial and stromal immune cell counts for the PR, CR and healthy donor tissues (**Figure 4**), and not for the NR group as this would be uninformative due to the overall low cell counts. This analysis shows that there are strong correlations between the number of infiltrating CD8$^+$ T cells and Th cells, as well as between the different types of myeloid cells; not only within a tissue segment (epithelium or stroma) but also between both tissue segments in healthy vulva and in complete responders (**Figure 4**). Importantly, there also is a strong correlation between the number of myeloid cells and CD8$^+$ T cells (healthy, CR) and Th1 cells (CR), suggesting a coordinated immune infiltration of T cells and myeloid cells in both healthy vulvar tissue and in vHSIL of patients who will respond well to therapeutic vaccination. In contrast, there is no or a negative correlation between the vHSIL-infiltrating T cells and myeloid cells in patients with a therapeutic vaccine-induced PR (**Figure 4**), suggesting that either T cells or myeloid cells are underrepresented in the pre-vaccination vHSIL immune microenvironment of PR patients.

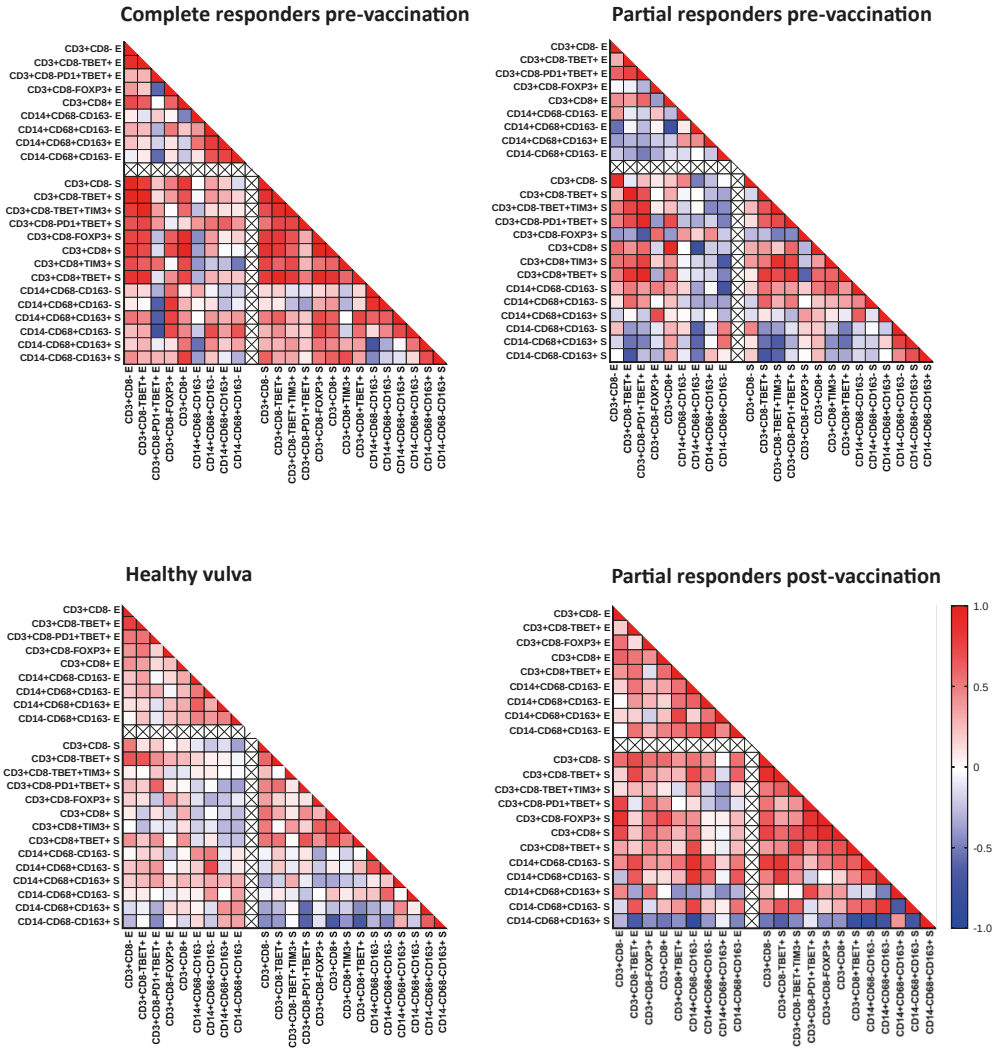

Figure 4. Correlation between the absolute numbers of tissue infiltrating T cells and myeloid cells in the pre- and post-treatment vHSIL biopsies and in healthy vulvar tissue.

Non-parametric Spearman r correlation analysis (two-tailed) was performed to analyze the co-infiltration of the indicated different immune cell subtypes in the epithelium (E) and stroma (S) and is shown in a heatmap for healthy vulvar tissue (n=27), pre-vaccination complete responder vHSIL patients (n=7) and partial responder vHSIL patients (n=10) as well as post-vaccination partial responder vHSIL patients (n=9).

Therapeutic vaccination does not overcome a "cold" low-infiltrated immune microenvironment

Three months post-vaccination all vHSIL patient were re-biopsied, except for 3 CR patients whom already reached complete response at three months follow-up, and for one NR and one PR patient of whom no post-vaccination biopsy material was available. Consequently, we were able to analyze the post-vaccination biopsies of 11 NR patients, 9 PR patients and 4 CR patients in the same manner as the pre-vaccination biopsies were analyzed. This revealed a strong increase in the number of $CD3^+CD8^-Tbet^+$ Th cells and a decrease in Tregs **(Figures 3b and 3c, Supplemental File 9)**, as well as a marked increase in CD14+ inflammatory myeloid cells and decreased numbers of M2 macrophages (**Figure 3b and 3c, Supplemental File 9**) in the vHSILs of patients with a PR or CR after vaccination. Notably, not only was the number of $CD14^+$ inflammatory myeloid cells increased, but also the proportion of $CD14^+$ cells expressing HLA-DR **(Supplemental File 7),** suggesting that these cells provide local help to the activation of the Th1 response. While the vHSILs of NR patients displayed only minor changes in these subsets (**Figure 3b and 3c, Supplemental File 9**), vaccination improved the coordinated immune infiltration of T cells and $CD14^+$ myeloid cells in PR patients **(Figure 4).** Last but not least, whereas the vHSIL of CR patients displayed both intraepithelial and stromal CD8+ T cell infiltration after vaccination, similar to what is seen in healthy vulvar tissue, the vHSIL of PR patients did not (**Figures 3b and 3c**). Notably, 2 out of 3 CR patients who could not be analyzed because their vHSIL disappeared within 3 months follow-up, already displayed high numbers of $Tbet^+$ Th cells (79 respectively 460 cells/mm2 stroma), $CD8^+$ T cells (44 respectively 107 cells/mm2 stroma), $CD14^+$ inflammatory myeloid cells (316 respectively 546 cells/mm2 stroma).

We have previously shown that patients with a CR displayed an overall stronger systemic IFNγ-associated proliferative response after vaccination[21], and this was also observed after 2 or 4 vaccinations in the currently selected cohort when the average production of IFNγ to all peptide pools of all patients in the groups was compared (**Figure 5a**), and when the average IFNγ production was depicted as the median of the maximal IFNγ production after either 2 or 4 vaccinations to all 6 E6 and E7 peptide pools per patient (**Figure 5b**). In order to understand the relative differences in immune infiltration and vaccine-induced T cell response between NR, PR and CR patients, we z-transformed the data of those immune cell types of which the counts significantly differed between the patient groups either pre- or post-vaccination, as well as that of the vaccine-specific IFNγ production (**Figure 5cd**). This revealed a propensity

of clinical responders to have pre-existing stromal infiltration with $CD4^+$ T cells (CD3+CD8-) and $CD14^+$ inflammatory myeloid cells. Furthermore, it suggests that in case a $CD14^+$ inflammatory myeloid cell infiltration is already present a strong vaccine-induced immune response is not required (**Figure 5c**). This profile was even more clear after vaccination, where clinical responsiveness was clearly correlated with the intraepithelial and stromal presence of type 1 $CD4^+$ T cells ($CD3^+CD8^-Tbet^+$) and $CD14^+$ inflammatory myeloid cells lacking the expression of CD163 as well as the relative absence of Tregs (**Figure 5d**). The absence of such a coordinated response before vaccination and the failure to alter this by vaccination, explains why some of the patients with a strong vaccine-induced T cell response still displayed a NR. Thus a generally strong and coordinated immune infiltration present already before or after vaccination in the TME by type 1 $CD4^+$ T cells and $CD14^+$ inflammatory myeloid cells was associated with a better clinical response to vaccination.

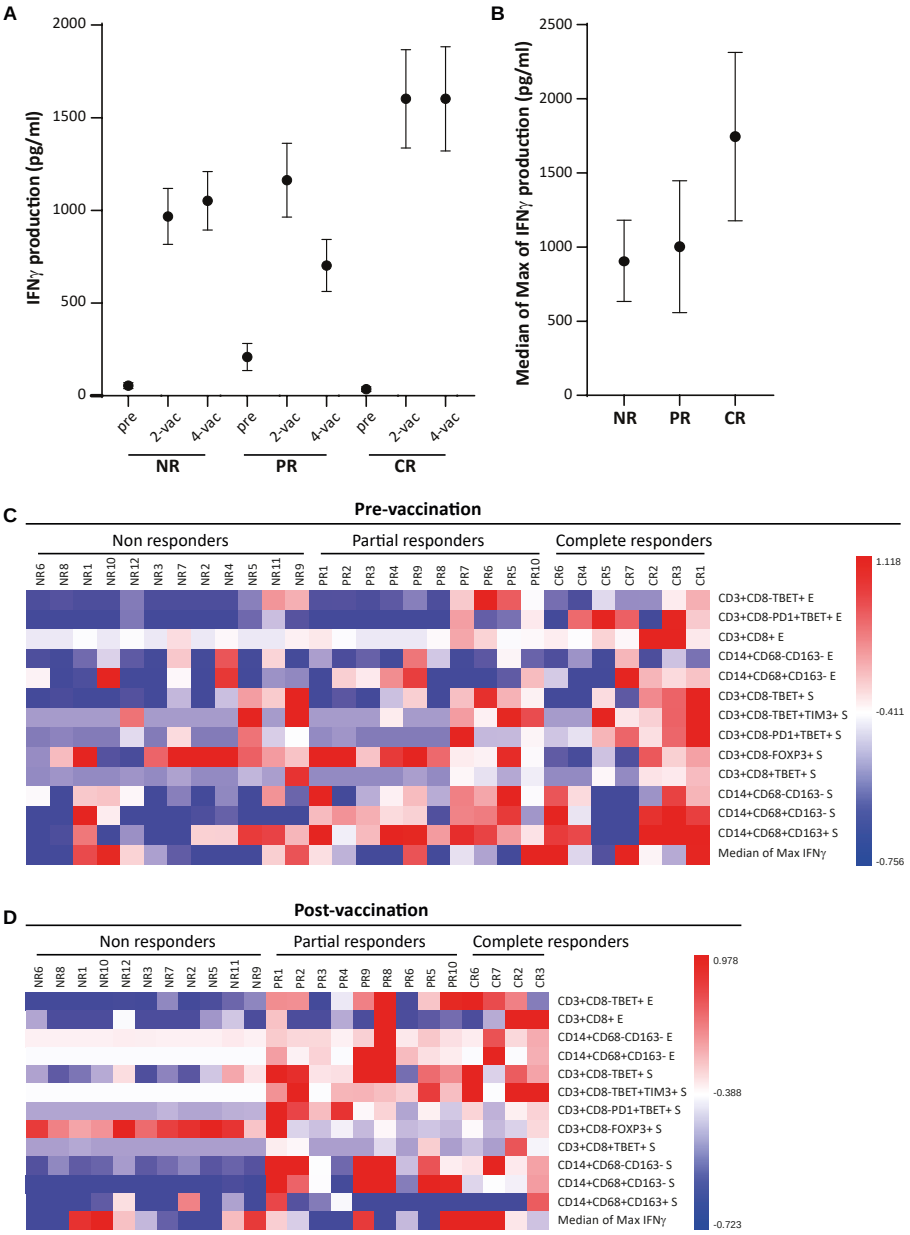

Figure 5. Immune profile of non-, partial- and complete responders bases on the relative infiltration of significantly different immune cell subtypes and HPV-specific T cell reactivity.

*The strength of the vaccine-induced HPV16-specific T cell response present in PBMC as measured by the production of IFNγ in the supernatant of PBMC stimulated with 6 different E6 and E7 peptide pools for clinical non-responders (NR), partial responders (PR) and complete responders (CR) as determined previously by cytokine bead array[20] is depicted as **A**) the mean ± SEM of all patients to all 6 peptide pools*

*tested, before and after 2 and 4 vaccinations; and **B**) the Median of Max calculated by taking the median of the highest responses to each peptide pool after 2 or 4 vaccinations. Shown is the mean ± SEM of all medians per group. **C** and **D**) The cell counts of all immune subsets of which the median cell count exceeded the threshold of ≥ 10 cells/mm2 and the numbers significantly differed between at least two of the patient groups (NR, PR, CR) either before vaccination (C) or after vaccination (D) as well as the Median of Max of IFNγ production as determined by cytometric bead array are depicted after the data was z-transformed to enable comparison of relative differences.*

Discussion

Our aim was to investigate if the immunological make up of HPV16-induced vHSIL was of influence on the clinical response of patients to an HPV16 SLP vaccine, shown to be active in two separate trials.[19, 21] Our study is the first to show that a coordinated immune infiltration by activated type 1 $CD8^+$ and T helper cells as well as HLA-DR^+CD14^+ myeloid cells is associated with a complete regression of vHSIL after vaccination. In a previous study, no difference was found in the numbers of pre-treatment vHSIL-infiltrating $CD4^+$ and $CD8^+$ T cells between patients with or without a complete clinical response after vaccination with an HPV16-E6E7L2 fusion protein vaccine.[29] This can be explained by the fact that these patients were pre-treated with imiquimod[29], which is known to induce strong local inflammation[30] that is reflected by infiltration with $CD4^+$ and $CD8^+$ T cells, activated DCs and macrophages[31], thereby recreating the desired immune microenvironment. But also because no functional assessment of the infiltrating T cells was performed, while our data clearly point at the role of $CD4^+$ $Tbet^+$ (type 1) Th cells. An impact of the pre-existing immune microenvironment on clinical outcome was also not found in cervical HSIL patients vaccinated with the HPV16/18 vaccine VGX-3100, but here only the number of $CD8^+$ T cells and Tregs was assessed[25] whereas it is known that also $CD14^+$ inflammatory myeloid cells are associated with better prognosis in cervical cancer[17] and as such are likely to play a similar role in its precursors. A coordinated response of T cells and inflammatory myeloid cells was also found to be required for the regression of tumors in the HPV16-positive tumor mouse models TC-1 and C3.[32] Last but not least, we used software that performed automatic tissue segmentation and cell phenotyping, enabling the analysis of the entire tissue slide thereby precluding selection bias of analyzed areas, and also preventing potential inter-observer variation.

Our analyses revealed that the pre-existing vHSIL-immune infiltrate of complete responders resembled that found in healthy vulvar tissue, whereas the immune infiltrate in vHSIL of PR and NR patients clearly differed. The vHSIL of NR

patients showed an overall low immune cell infiltration except for Tregs which were most abundant in this patient group, indicating that these lesions lacked inflammation and were immune suppressed, hence they can be branded as relatively immune deserted/immunosuppressed.[10] Since healthy vulvar tissue comprises an actively inflamed immune microenvironment, the absence of it in the TME of NR must be labeled as aberrant. The underlying mechanism for this is currently unknown but potentially the answer can be found in the genomic instability of the lesions, which is often found on top of the expression of the HPV16 oncoproteins[33-35], and has been related to immune evasion and reduced response to immunotherapy[36]. Analyses of the post-vaccination samples at 3 months of follow-up made it clear that therapeutic vaccination was incapable of overcoming the "cold" local microenvironment that is present in non-responders. The intrinsic or extrinsic escape mechanism underlying this incapacity to attract immune effector cells is part of future studies.

While the vHSIL of partial responders generally was infiltrated more densely with immune cells, a correlation analysis of the pre-existing immune cell infiltrate revealed that there was either no or a negative correlation between the numbers of vHSIL-infiltrating T cells and myeloid cells in this PR group. Some of them were relatively strongly infiltrated with T cells, a phenotype previously found to be correlated with partial responses of vHSIL after vaccination[37], whereas others displayed relatively high levels of myeloid cells only. After vaccination, strong increases in both type 1 Th cells and HLA class II-positive inflammatory macrophages were observed in the vHSIL of patients with a PR or CR at 12 months of follow up. This coincided with lower numbers of Tregs and M2 macrophages. Hence, therapeutic vaccination can incite and modulate inflamed lesions so that the immune infiltration becomes more coordinated and the effector cells increase to similar or higher numbers when compared to healthy vulvar tissue. In this aspect it does not differ from other T cell based approaches, including adoptive T cell transfer[38] and checkpoint blockade[10, 39] all of which have the best possible clinical impact when a tumor is inflamed or hot before start of therapy. The HPV16 SLP vaccine did not increase the numbers of vHSIL-infiltrating $CD8^+$ T cells, which were present already in the vHSIL that became a CR but not in vHSIL ending up as PR.

Finally, several trials with therapeutic vaccines against HPV-induced HSIL lesions have reported overall high immunogenicity of the vaccine but complete clinical responses in only part of the treated subjects.[19-22, 29, 37, 40] The data of this study suggests that the HSIL microenvironment has an impact on the vaccine-

induced clinical outcome and as such calls for the prospective validation of the combination of $CD4^+$ cells, $Tbet^+$ cells and $CD14^+$ myeloid cells as predictive biomarkers for clinical response of HSIL to therapeutic vaccination. These biomarkers can easily be applied in routine diagnostics, as they only require routinely taken FFPE tissue and regular single immunohistochemical stainings. The combination of multiple biomarkers is likely to increase the sensitivity of the prediction tool.[41] Furthermore, our data strongly suggest that the efficacy of therapeutic vaccines in this patient group can be increased when it is combined with other drugs that induce local acute inflammation, to support the infiltration of vaccine-activated T cells and inflammatory myeloid cells. Hence, our findings show that the current paradigm of personalized cancer immunotherapy also applies to therapeutic vaccines for the treatment of patients with virally induced lesions as well as provides a foundation for future combination therapy studies.

Supplemental Files

Supplemental File 1. Design T cell panel, antibodies and detection method per marker.

Marker	Primary antibody clone and company	Primary antibody isotype	Secondary antibody	Detection method
PD-1	D4W2J Cell Signaling Technology	Rabbit IgG	Poly-HRP and Opal 570	Opal tyramide signal amplification
Tbet	D6N8B XP Cell Signaling Technology	Rabbit IgG	Poly-HRP and Opal 520	Opal tyramide signal amplification
FoxP3	236A/E7 Invitrogen ThermoFisher	Mouse IgG1	CF goat anti mouse IgG1 633	Secondary antibody fluorochrome labelled
CD8	4B11 Novocastra	Mouse IgG2b	Alexa goat anti mouse IgG2b 647	Secondary antibody fluorochrome labelled
Tim3	D5D5R XP Cell Signaling Technology	Rabbit IgG	Alexa goat anti rabbit IgG 680	Secondary antibody fluorochrome labelled
CD3	D7A6E Cell Signaling Technology, directly labelled with Alexa 594	Rabbit IgG	-	Directly fluorochrome labelled primary antibody
DAPI	ThermoFisher	-	-	Fluorescent probe

Supplemental File 2. Design myeloid cell panel, antibodies and detection method per marker.

Marker	Primary antibody clone and company	Primary antibody isotype	Secondary antibody	Detection method
PD-L1	SP142 Spring Bioscience	Rabbit IgG	Poly-HRP and Opal 520	Opal tyramide signal amplification
CD14	D7A2T Cell Signaling Technology	Rabbit IgG	CF donkey anti rabbit IgG 633	Secondary antibody fluorochrome labelled
CD33	PWS44 Novocastra	Mouse IgG2b	Alexa goat anti mouse IgG2b 647	Secondary antibody fluorochrome labelled
CD163	10D6 Invitrogen ThermoFisher	Mouse IgG1	CF goat anti mouse IgG1 680	Secondary antibody fluorochrome labelled
CD11c	EP1347Y Abcam, directly labelled with Alexa 546	Rabbit IgG	-	Directly fluorochrome labelled primary antibody
CD68	D4B9C XP Cell Signaling Technology, directly labelled with Alexa 594	Rabbit IgG	-	Directly fluorochrome labelled primary antibody
DAPI	ThermoFisher	-	-	Fluorescent probe

Supplemental File 3. Inform analyses.

A

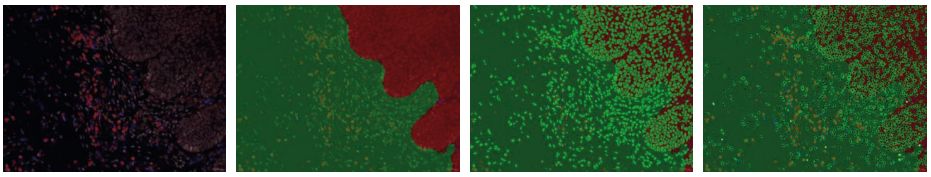

1 2 3 4

A) Multispectral immunofluorescence image analysis workflow with inForm , representative example of a subanalysis . InForm uses a stepwise training approach, each step adding a layer of differentiation.

Step 1: Signal extraction	(example subanalysis here shows CD68 in red, CD163 in blue)
Step 2: Tissue segmentation	(epithelium in red, stroma in green)
Step 3: Cell segmentation	(cells are marked in light green)
Step 4: Cell phenotyping	(CD68 CD163 cells are assigned a red dot, CD68 CD163 + cells a blue dot, CD68 CD163 cells a yellow dot, and CD68 CD163 cells a black dot)

B

T cell panel		Myeloid cell panel	
Subanalysis 1:		Subanalysis 1:	
$CD3^+CD8^-FoxP3^-$	(T helper cell)	$CD68^+CD163^-$	(M1 macrophage)
$CD3^+CD8^+FoxP3^-$	($CD8^+$ T cell)	$CD68^+CD163^+$	(M2 macrophage)
$CD3^+CD8^-FoxP3^+$	(regulatory T cell)	$CD68^-CD163^+$	($CD163^+$ non-macrophage)
$CD3^-CD8^-FoxP3^-$	(no T cell)	$CD68^-CD163^-$	(non-macrophage)
Subanalysis 2:		Subanalysis 2:	
$Tbet^+$	(IFNγ producing T cell)	$CD11c^+CD14^-$	(dendritic cell, DC)
$Tbet^-$	($Tbet^-$ T cell)	$CD11c^+CD14^+$	(inflammatory DC)
		$CD11c^-CD14^+$	(inflammatory myeloid cell)
Subanalysis 3:		$CD11c^-CD14^-$	($CD11c^-$ and $CD14^-$ myeloid cell)
$PD1^+$	(activated PD1 expressing T cell)		
$PD1^-$	($PD1^-$ T cell)	Subanalysis 3:	
		$CD33^+PDL1^-$	(immature myeloid cell)
Subanalysis 4:		$CD33^-PDL1^+$	(mature myeloid cell expressing PDL1)
$Tim3^+$	(activated Tim3 expressing T cell)	$CD33^-PDL1^-$	($CD33^-$ and $PDL1^-$ myeloid cell)
$Tim3^-$	($Tim3^-$ T cells)		

B) Subanalyses of the T cell and myeloid cell panel as used in inForm . The full seven marker panels were divided into multiple subanalyses , to preclude the exclusion of possible relevant phenotypes. Subsequently, the output of the multiple subanalyses were merged per cell based on X,Y positions to obtain the full seven marker expression profile of each cell.

Supplemental File 4. Examples of immune cell subtypes analyzed.

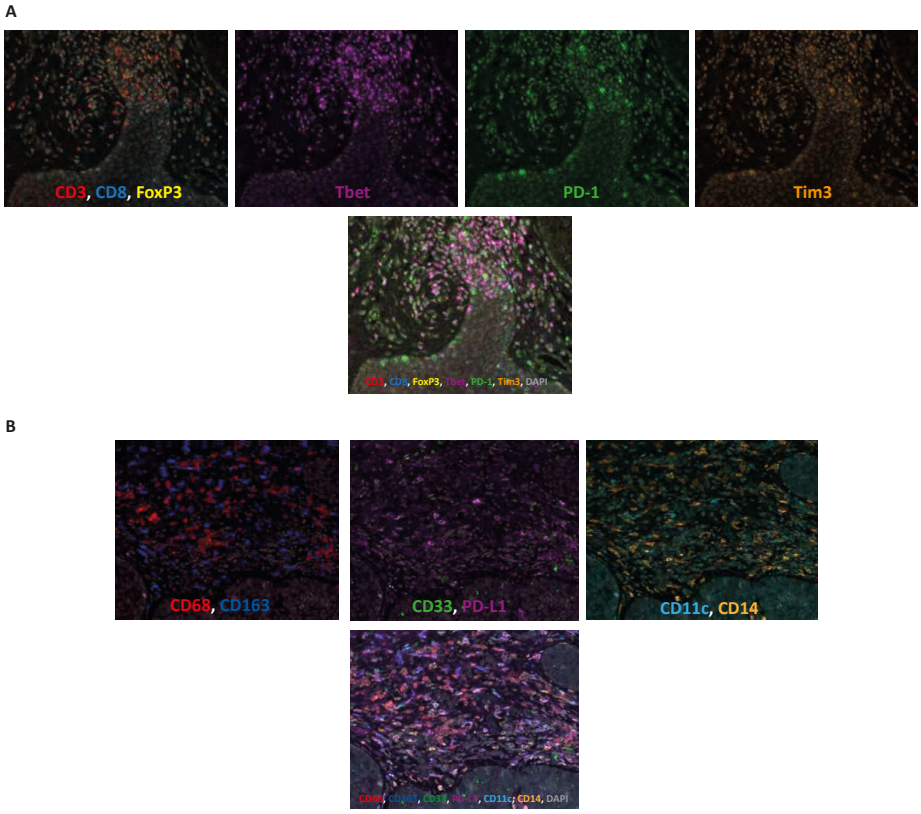

A) Analysis of the T cell panel consisted of four sub-analyses; first CD3, CD8, FoxP3 positivity was assessed, secondly Tbet, thirdly PD-1, and fourthly Tim3.
B) Analysis of the myeloid cell panel consisted of three sub-analyses: first CD68 and CD163 positivity was assessed,secondly CD33 and PD-L1, and thirdly CD11c and CD14.

Supplemental File 5. Descriptive statistics of immune cells in healthy vulvar tissue.

Immune cell phenotype	Number of cells/mm2 epithelium (median with 95% CI)	Number of cells/mm2 stroma (median with 95% CI)
CD3+CD8-FoxP3-	57.62 (13.81-123)	43.49 (8.67-70.51)
CD3+CD8+FoxP3-	8.52 (3.49-29.13)	17.38 (6.33-21.87)
CD3+CD8-FoxP3+	2.98 (0.81-7.15)	5.23 (1.09-9.90)
Tbet+	100.6 (56.59-176)	106.9 (29.93-139)
PD1+	44.89 (22.53-92.33)	32.10 (23.48-47.29)
Tim3+	14.76 (10.44-19.52)	23.48 (17.31-31.79)
CD68+CD163-	5.20 (3.59-18.59)	52.89 (17.07-106)
CD68-CD163+	0.00 (0.00-1.99)	13.45 (9.53-34.62)
CD68+CD163+	3.78 (1.79-22.32)	96.74 (67.84-140)
CD11c+CD14-	0.54 (0.00-1.73)	11.62 (4.77-20.59)
CD11c-CD14+	50.97 (17.87-99.03)	286.60 (196-526)
CD11c+CD14+	0.00 (0.00-0.00)	0.88 (0.00-3.32)
CD33+PDL1-	16.92 (5.38-35.73)	39.23 (28.22-75.49)
CD33-PDL1+	3.87 (1.20-20.72)	25.33 (9.97-67.06)

N=15 healthy vulvar tissue samples; CI=confidence interval

Supplemental File 6. Descriptive statistics of immune cells in vHSIL as one group and based on clinical response after vaccination.

Immune cell phenotype	Number of cells/mm2 epithelium (median with 95% CI)				Number of cells/mm2 stroma (median with 95% CI)			
	vHSIL all	NR	PR	CR	vHSIL all	NR	PR	CR
CD3+CD8-FoxP3-	25.46 (5.94-49.85)	7.45 (5.51-38.53)	28.03 (2.31-97.00)	41.64 (8.28-98.45)	12.39 (4.00-33.32)	8.23 (2.21-20.44)	7.47 (1.74-81.40)	37.60 (11.36-72.40)
CD3+CD8+FoxP3-	2.32 (0.00-5.52)	0.00 (0.00-5.97)	2.32 (0.00-12.85)	5.52 (1.50-229)	11.89 (3.91-29.12)	7.55 (3.78-27.31)	13.77 (1.74-35.73)	65.69 (1.34-324)
CD3+CD8-FoxP3+	7.51 (4.47-13.19)	11.30 (4.29-13.86)	8.52 (3.51-23.20)	6.90 (2.86-36.44)	47.93 (23.69-90.40)	51.18 (8.84-112)	69.32 (23.69-102)	22.04 (4.01-99.34)
Tbet+	27.90 (4.14-50.84)	8.66 (0.79-28.16)	33.16 (3.35-90.43)	50.84 (4.14-304.5)	105.20 (37.84-159)	61.33 (12.92-155)	126.6 (22.60-300)	158.70 (14.56-722)
PD1+	20.70 (7.08-50.75)	10.46 (1.19-55.45)	10.21 (0.00-38.78)	150 (20.70-433)	52.15 (34.72-145)	86.10 (24.72-145)	37.03 (9.91-135)	184.90 (29.12-282)
Tim3+	3.70 (2.36-11.59)	3.28 (0.77-15.05)	4.20 (0.91-20.56)	11.46 (0.00-39.21)	28.31 (17.49-98.97)	56.08 (3.59-121)	20.80 (6.95-101)	18.59 (7.66-179)
CD68+CD163-	15.33 (6.88-25.02)	11.22 (3.91-25.02)	17.27 (6.88-26.32)	14.37 (4.60-108)	153.70 (49.05-219)	74.35 (30.01-219)	175.2 (85.51-332)	162.70 (30.05-1562)
CD68-CD163+	0.00 (0.00-0.270)	0.00 (0.00-1.78)	0.00 (0.00-0.46)	0.00 (0.00-6.27)	13.28 (7.14-30.59)	29.73 (1.91-84.54)	12.61 (3.56-30.59)	10.33 (0.00-43.59)
CD68+CD163+	1.19 (0.00-6.90)	1.15 (0.00-6.90)	1.29 (0.00-13.73)	3.89 (0.00-45.73)	253.5 (130-295)	155.50 (65.33-351)	272.2 (142-335)	216.90 (73.41-715)
CD11c+CD14-	1.88 (0.00-4.26)	0.84 (0.00-2.43)	8.67 (0.00-30.03)	3.34 (0.00-9.19)	27.60 (14.90-82.64)	20.58 (12.86-44.05)	96.41 (8.27-224)	51.49 (4.12-246)
CD11c-CD14+	8.36 (3.59-14.71)	3.91 (0.00-27.83)	9.19 (4.53-17.59)	11.68 (0.00-75.81)	228.5 (175-437)	188.60 (122-229)	410.7 (210-579)	496.80 (35.82-648)
CD11c+CD14+	0.00 (0.00-0.54)	0.00 (0.00-3.54)	0.00 (0.00-1.07)	0.00 (0.00-35.78)	10.84 (6.37-16.20)	9.24 (1.26-14.19)	11.98 (6.37-48.39)	12.56 (0.00-133)
CD33+PDL1-	11.73 (6.12-17.72)	13.68 (3.09-23.63)	10.00 (3.43-17.72)	20.22 (1.88-34.10)	63.03 (41.17-92.63)	63.09 (25.73-121)	62.11 (45.73-101)	81.04 (9.25-290)
CD33-PDL1+	5.44 (0.76-25.90)	15.71 (2.20-40.78)	0.38 (0.00-41.69)	5.44 (0.00-100)	53.75 (38.14-80.12)	32.11 (8.58-123)	58.47 (42.92-125)	54.43 (10.33-459)

vHSIL all (n=29); non-responders (NR, n=12); partial responders (PR, n=10); complete responders (CR, n=7); CI=confidence interval

Supplemental File 7. CD14+ inflammatory myeloid cells co-expressing HLA-DR, in pre- and postvaccination vHSIL and in healthy vulva.

A

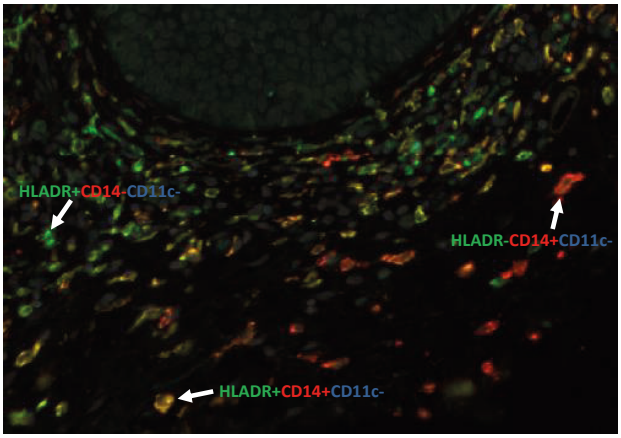

Example of HLA-DR expressing CD14+ myeloid cells in vHSIL. For this staining, a panel consisting of HLA-DR (clone TAL1B5, directly labelled with Alexa fluor 594), CD14 (clone D7A2T, indirectly detected with CF donkey anti rabbit IgG 633), CD11c (clone EP1347Y, directly labelled with Alexa fluor 546) and DAPI was designed.

B

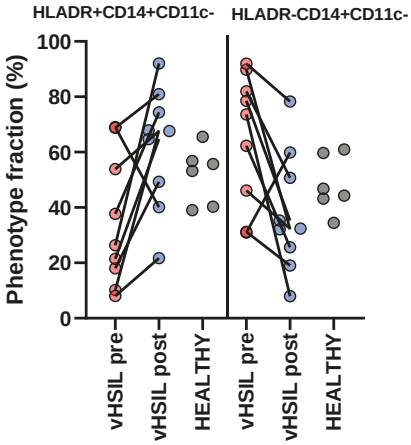

6 healthy vulva samples and the pre- and post-vaccination biopsies of 9 vHSIL patients (3 NR, 3 PR, 3 CR) were stained and analyzed with this panel. Samples for staining were selected based on high CD14+ cell counts. Upon vaccination, the fraction of CD14+ cells co-expressing HLA-DR increases.

Supplemental File 8. Almost all CD3+CD8-Foxp3- T cells co-express CD4.

A

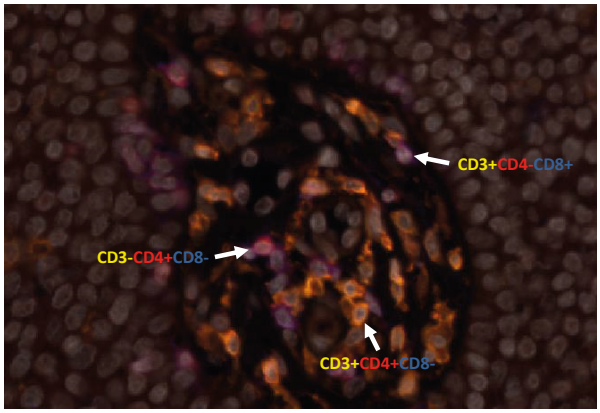

Example of CD3, CD4 and CD8 expression in a vHSIL biopsy. For this staining, a panel consisting of CD3 (clone D7A6E, directly labelled with Alexa fluor 594), CD4 (clone EPR6855, indirectly detected with Alexa fluor goat anti rabbit IgG 546), CD8 (clone 4B11, indirectly detected with Alexa fluor goat anti mouse IgG2b 647) and DAPI was designed.

B

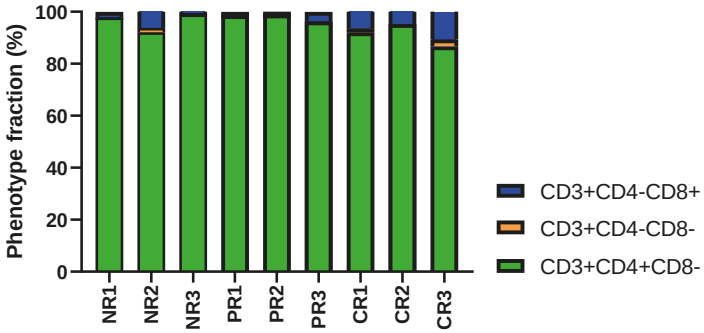

9 pre-vaccination vHSIL samples (3 NR, 3 PR, 3 CR) were stained and analyzed with the CD3, CD4, CD8, DAPI panel. Samples for staining were selected based on high CD3+CD8-Foxp3- cell counts. Of all CD3+CD8- cells, 99.1% was CD3+CD4+ (median, range 97-100%).

References

1. Galon J, Angell HK, Bedognetti D, Marincola FM. The continuum of cancer immunosurveillance: prognostic, predictive, and mechanistic signatures. Immunity. 2013;39(1):11-26.
2. Fridman WH, Pages F, Sautes-Fridman C, Galon J. The immune contexture in human tumours: impact on clinical outcome. Nat Rev Cancer. 2012;12(4):298-306.
3. Rosenberg SA, Restifo NP. Adoptive cell transfer as personalized immunotherapy for human cancer. Science. 2015;348(6230):62-8.
4. Fesnak AD, June CH, Levine BL. Engineered T cells: the promise and challenges of cancer immunotherapy. Nat Rev Cancer. 2016;16(9):566-81.
5. Sharma P, Allison JPJS. The future of immune checkpoint therapy. Science. 2015;348(6230):56-61.
6. Whiteside TL, Demaria S, Rodriguez-Ruiz ME, Zarour HM, Melero I. Emerging Opportunities and Challenges in Cancer Immunotherapy. Clin Cancer Res. 2016;22(8):1845-55.
7. Hegde PS, Karanikas V, Evers S. The Where, the When, and the How of Immune Monitoring for Cancer Immunotherapies in the Era of Checkpoint Inhibition. Clin Cancer Res. 2016;22(8):1865-74.
8. Tumeh PC, Harview CL, Yearley JH, Shintaku IP, Taylor EJ, Robert L, et al. PD-1 blockade induces responses by inhibiting adaptive immune resistance. Nature. 2014;515(7528):568-71.
9. van der Burg SH. Correlates of immune and clinical activity of novel cancer vaccines. Sem Immunol. 2018;39:119-36.
10. Galon J, Bruni D. Approaches to treat immune hot, altered and cold tumours with combination immunotherapies. Nat Rev Drug Discov. 2019;18(3):197-218.
11. Chen DS, Mellman I. Elements of cancer immunity and the cancer-immune set point. Nature. 2017;541(7637):321-30.
12. McLaughlin-Drubin ME, Munger K. Viruses associated with human cancer. Biochim Biophys Acta. 2008;1782(3):127-50.
13. Welters MJ, Kenter GG, Piersma SJ, Vloon AP, Lowik MJ, Berends-van der Meer DM, et al. Induction of tumor-specific CD4+ and CD8+ T-cell immunity in cervical cancer patients by a human papillomavirus type 16 E6 and E7 long peptides vaccine. Clin Cancer Res. 2008;14(1):178-87.
14. Kenter GG, Welters MJ, Valentijn ARP, Löwik MJ, Berends-van der Meer DM, Vloon AP, et al. Phase I immunotherapeutic trial with long peptides spanning the E6 and E7 sequences of high-risk human papillomavirus 16 in end-stage cervical cancer patients shows low toxicity and robust immunogenicity. Clin Cancer Res. 2008;14(1):169-77.
15. Bagarazzi ML, Yan J, Morrow MP, Shen X, Parker RL, Lee JC, et al. Immunotherapy against HPV16/18 generates potent TH1 and cytotoxic cellular immune responses. Sci Transl Med. 2012;4(155):155ra38.
16. Kim TJ, Jin HT, Hur SY, Yang HG, Seo YB, Hong SR, et al. Clearance of persistent HPV infection and cervical lesion by therapeutic DNA vaccine in CIN3 patients. Nat Comm. 2014;5:5317.
17. de Vos van Steenwijk PJ, Ramwadhdoebe TH, Goedemans R, Doorduijn EM, van Ham JJ, Gorter A, et al. Tumor-infiltrating CD14-positive myeloid cells and CD8-positive T-cells prolong survival in patients with cervical carcinoma. Int J Cancer. 2013;133(12):2884-94.
18. de Vos van Steenwijk PJ, van Poelgeest MI, Ramwadhdoebe TH, Lowik MJ, Berends-van der Meer DM, van der Minne CE, et al. The long-term immune response after HPV16 peptide vaccination in women with low-grade pre-malignant disorders of the uterine cervix: a placebo-controlled phase II study. Cancer Immunol Immunother. 2014;63(2):147-60.
19. Kenter GG, Welters MJ, Valentijn AR, Lowik MJ, Berends-van der Meer DM, Vloon AP, et al. Vaccination against HPV-16 oncoproteins for vulvar intraepithelial neoplasia. N Engl J Med. 2009;361(19):1838-47.
20. Welters MJ, Kenter GG, de Vos van Steenwijk PJ, Lowik MJ, Berends-van der Meer DM, Essahsah F, et al. Success or failure of vaccination for HPV16-positive vulvar lesions correlates with kinetics and phenotype of induced T-cell responses. Proc Natl Acad Sci U S A. 2010;107(26):11895-9.
21. van Poelgeest MI, Welters MJ, Vermeij R, Stynenbosch LF, Loof NM, Berends-van der Meer DM, et al. Vaccination against Oncoproteins of HPV16 for Noninvasive Vulvar/Vaginal Lesions: Lesion Clearance Is Related to the Strength of the T-Cell Response. Clin Cancer Res. 2016;22(10):2342-50.
22. Trimble CL, Morrow MP, Kraynyak KA, Shen X, Dallas M, Yan J, et al. Safety, efficacy, and immunogenicity of VGX-3100, a therapeutic synthetic DNA vaccine targeting human papillomavirus 16 and 18 E6 and E7 proteins for cervical intraepithelial neoplasia 2/3: a randomised, double-blind, placebo-controlled phase 2b trial. Lancet. 2015;386(10008):2078-88.

23. Massarelli E, William W, Johnson F, Kies M, Ferrarotto R, Guo M, et al. Combining Immune Checkpoint Blockade and Tumor-Specific Vaccine for Patients With Incurable Human Papillomavirus 16-Related Cancer: A Phase 2 Clinical Trial. JAMA Oncol. 2018.
24. Melief CJM, Welters MJP, Vergote I, Kroep JR, Kenter GG, Ottevanger PB, et al. Strong vaccine responses during chemotherapy are associated with prolonged cancer survival. Nature. 2019.
25. Morrow MP, Kraynyak KA, Sylvester AJ, Dallas M, Knoblock D, Boyer JD, et al. Clinical and Immunologic Biomarkers for Histologic Regression of High-Grade Cervical Dysplasia and Clearance of HPV16 and HPV18 after Immunotherapy. Clin Cancer Res. 2018;24(2):276-94.
26. van Esch EM, van Poelgeest MI, Kouwenberg S, Osse EM, Trimbos JB, Fleuren GJ, et al. Expression of coinhibitory receptors on T cells in the microenvironment of usual vulvar intraepithelial neoplasia is related to proinflammatory effector T cells and an increased recurrence-free survival. Int J Cancer. 2015;136(4):E95-106.
27. van Esch EM, van Poelgeest MI, Trimbos JB, Fleuren GJ, Jordanova ES, van der Burg SH. Intraepithelial macrophage infiltration is related to a high number of regulatory T cells and promotes a progressive course of HPV-induced vulvar neoplasia. Int J Cancer. 2015;136(4):E85-94.
28. Ijsselsteijn ME, Brouwer TP, Abdulrahman Z, Reidy E, Ramalheiro A, Heeren AM, et al. Cancer immunophenotyping by seven-colour multispectral imaging without tyramide signal amplification. J Pathol Clin Res. 2019;5(1):3-11.
29. Daayana S, Elkord E, Winters U, Pawlita M, Roden R, Stern PL, et al. Phase II trial of imiquimod and HPV therapeutic vaccination in patients with vulval intraepithelial neoplasia. Br J Cancer. 2010;102(7):1129-36.
30. Mauldin IS, Wages NA, Stowman AM, Wang E, Olson WC, Deacon DH, et al. Topical treatment of melanoma metastases with imiquimod, plus administration of a cancer vaccine, promotes immune signatures in the metastases. Cancer Immunol Immunother. 2016;65(10):1201-12.
31. Barnetson RS, Satchell A, Zhuang L, Slade HB, Halliday GM. Imiquimod induced regression of clinically diagnosed superficial basal cell carcinoma is associated with early infiltration by CD4 T cells and dendritic cells. Clin Exp Dermatol. 2004;29(6):639-43.
32. van der Sluis TC, Sluijter M, van Duikeren S, West BL, Melief CJ, Arens R, et al. Therapeutic Peptide Vaccine-Induced CD8 T Cells Strongly Modulate Intratumoral Macrophages Required for Tumor Regression. Cancer Immunol Res. 2015;3(9):1042-51.
33. Aulmann S, Schleibaum J, Penzel R, Schirmacher P, Gebauer G, Sinn HP. Gains of chromosome region 3q26 in intraepithelial neoplasia and invasive squamous cell carcinoma of the vulva are frequent and independent of HPV status. J Clin Pathol. 2008;61(9):1034-7.
34. Bryndorf T, Kirchhoff M, Larsen J, Andreasson B, Bjerregaard B, Westh H, et al. The most common chromosome aberration detected by high-resolution comparative genomic hybridization in vulvar intraepithelial neoplasia is not seen in vulvar squamous cell carcinoma. Cytogenet Genome Res. 2004;106(1):43-8.
35. Rosenthal AN, Ryan A, Hopster D, Surentheran T, Jacobs IJ. High frequency of loss of heterozygosity in vulval intraepithelial neoplasia (VIN) is associated with invasive vulval squamous cell carcinoma (VSCC). Int J Cancer. 2001;94(6):896-900.
36. Davoli T, Uno H, Wooten EC, Elledge SJ. Tumor aneuploidy correlates with markers of immune evasion and with reduced response to immunotherapy. Science. 2017;355(6322).
37. Davidson EJ, Boswell CM, Sehr P, Pawlita M, Tomlinson AE, McVey RJ, et al. Immunological and clinical responses in women with vulval intraepithelial neoplasia vaccinated with a vaccinia virus encoding human papillomavirus 16/18 oncoproteins. Cancer Res. 2003;63(18):6032-41.
38. Melief SM, Visconti VV, Visser M, van Diepen M, Kapiteijn EH, van den Berg JH, et al. Long-term Survival and Clinical Benefit from Adoptive T-cell Transfer in Stage IV Melanoma Patients Is Determined by a Four-Parameter Tumor Immune Signature. Cancer Immunol Res. 2017;5(2):170-9.
39. Gajewski TF. The Next Hurdle in Cancer Immunotherapy: Overcoming the Non-T-Cell-Inflamed Tumor Microenvironment. Semin Oncol. 2015;42(4):663-71.
40. Baldwin PJ, van der Burg SH, Boswell CM, Offringa R, Hickling JK, Dobson J, et al. Vaccinia-expressed human papillomavirus 16 and 18 e6 and e7 as a therapeutic vaccination for vulval and vaginal intraepithelial neoplasia. Clin Cancer Res. 2003;9(14):5205-13.
41. Signorelli D, Giannatempo P, Grazia G, Aiello MM, Bertolini F, Mirabile A, et al. Patients Selection for Immunotherapy in Solid Tumors: Overcome the Naïve Vision of a Single Biomarker. Biomed Res Int. 2019;9056417.